Evolving fabric and its impact on the shearing behaviour of a compacted clayey silt exposed to drying-wetting cycles

A. Azizi & G. Musso
Department of Structural, Building and Geotechnical Engineering, Politecnico di Torino, Torino, Italy

C. Jommi
Department of Geoscience and Engineering, Delft University of Technology, Delft, the Netherlands
Department of Civil and Environmental Engineering, Politecnico di Milano, Milano, Italy

R. M. Cosentini
Department of Civil Engineering and Architecture, Università di Pavia, Pavia, Italy

ABSTRACT: The fabric and the hydro-mechanical behaviour of compacted clayey silt samples were investigated before and after drying-wetting cycles. Drying-wetting cycles changed the soil fabric by increasing the macro-porosity, while the total void ratio remained almost constant. The cycled samples were more compressible than the original ones and experienced a smaller decrease of suction during shearing at constant water content. The higher compressibility is associated to a more evident reduction of macro-porosity. The smaller suction decrease is reproduced with a double structure water retention model accounting for changes in macro-porosity during shearing. Cycled samples mobilised higher strength and showed a higher dilatancy than original samples sheared at the same initial total stress and suction; furthermore, dilatancy increased with suction for both fabrics. The Li and Dafalias stress-dilatancy relationship, formulated in terms of a macro-structural Bishop stress and accounting for a suction dependency, allowed reproducing the experimental results accurately.

1 INTRODUCTION

Earth structures are exposed continuously to interaction with the atmosphere, due to yearly cycles of relative humidity (dry against wet seasons, temperature oscillations) and precipitations (rainfalls and snowfalls). Such interaction causes hydraulic stresses, which are particularly intense at the superficial layers of levees and embankments.

The hydro-mechanical behaviour of the soil used in the construction is affected by these events, leading to different performance a few years after construction. For compacted soils interacting with the atmosphere, the saturated hydraulic conductivity was found to increase and the air-entry of water retention curve to reduce over time (Benson et al. 2007). Changes in the hydro-mechanical behaviour are very important for soils of medium to high plasticity (Albrecht & Benson 2001). Nevertheless, even non-plastic clayey silts, which neither crack nor deform appreciably under hydraulic loads, can undergo significant changes in the hydro-mechanical response, which is related to fabric evolution (Azizi et al. 2018).

Scarce attention has been paid in the past to the impact of fabric changes induced by drying-wetting cycles on the shearing behaviour, although this is an important aspect too, related to the stability of earth constructions. The aim of the paper is to characterise the shearing behaviour under unsaturated conditions of a compacted clayey silt, tested both immediately after preparation and after drying-wetting cycles. The investigated material was collected at Viadana (North Italy) where it was used in the construction of an experimental embankment, aimed to study the impact of high water on the hydraulic protection structures of the Po river (Calabresi et al. 2013).

2 MATERIAL AND SAMPLE PREPARATION

The tested material is a non-plastic clayey silt. The specific gravity is G_s = 2.735, the liquid and plastic limits are 32.6% and 24.3%, respectively. The clay fraction (particle diameter $d \leq 2$ μm) is 20%, the silt fraction (2 μm < $d \leq 60$ μm) is 74% and the remaining fraction is fine sand ($d_{max} < 0.1$ μm).

The samples were prepared by static compaction, at an initial gravimetric water content w = 20% and a dry density ρ_d = 1680 kg/m^3. The void ratio at preparation was e = 0.66 and the degree of saturation was S_r = 83%. The dry soil powder was sprayed and hand-mixed with demineralized water according to the target water content, sealed in plastic bags and placed in a humid container for 48 hours allowing water content equilibration. The wet soil was placed in rigid moulds having a diameter of 50 mm (oedometer samples) or 38 mm (triaxial samples) and compacted to the desired density and height.

2.1 *Drying-wetting cycles*

After compaction, some samples were loaded with a small axial load (10 kPa) and left to rest on a rigid mesh, across which evaporation occurred. Drying

was imposed by exposing the samples to the laboratory environment (R.H. = 38.5%, T = 21°C; s = 129 MPa according to the psychrometric law). The average water content at equilibrium with the laboratory condition was w = 0.38%.

Wetting was imposed by introducing within the sample the mass of water required to regain the original water content. A drainage circuit connected to a water volume change indicator actuated by a pressure line allowed imbibition (Figure 1). The injection rate imposed during wetting (0.5 cm^3/h) was deliberately low to prevent possible damages due to high pressure and pressure gradients.

During the first drying-wetting cycles, the volume strains (shrinkage upon drying and swelling upon wetting) were not completely reversible, and shrinkage initially increased. After three cycles, the volume strains were mainly reversible and volume changes stabilised (Figure 2).

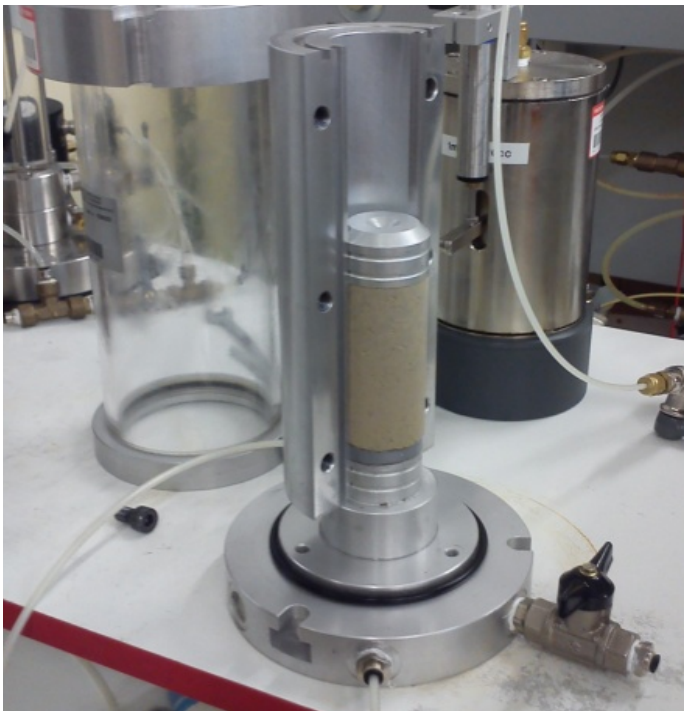

Figure 1. View of the rigid mould with sample, water line and volume change indicator.

3 FABRIC AND FABRIC EVOLUTION

The fabric was characterised through the Mercury Intrusion Porosimetry technique (MIP). Samples having different hydraulic and mechanical histories were characterised. To preserve their initial fabric, all samples were freeze-dried before the porosimetry tests (Delage and Pellerin, 1984). Four states were considered: after compaction (Original Fabric sample, OF), after six drying-wetting cycles (Cycled Fabric sample, CF), compacted and loaded in oedometer under a vertical stress σ_v = 100 kPa (loaded OF) and compacted, exposed to six drying-wetting cycles and loaded in oedometer conditions to σ_v = 100 kPa (loaded CF). The Pore Size Density (PSD) of these four samples is introduced in Figure 3.

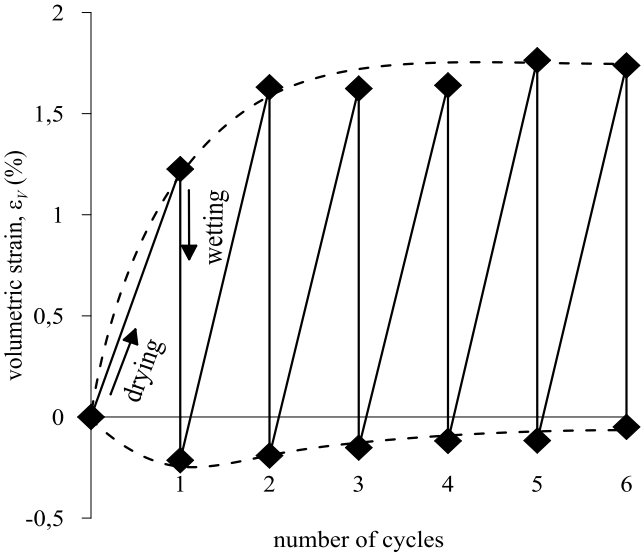

Figure 2. Volumetric strains during drying-wetting cycles.

According to Environmental Scanning Electron Microscope (ESEM) images, the fabric consists of silt grains and peds of clay particles. Smaller pores are assumed to be contained within the peds (intra-peds pores) while larger pores (macropores) are assumed to form the void space between peds and between the peds and the silt grains. The radius sizes corresponding to the major peaks in the PSD are chosen to separate the intra-peds pores from the macropores. This assumption allows identifying two structural levels: one related to the peds and the other one related to the macroscopic structure. The volume of the pores having a radius smaller than the threshold referred to the volume of solids measures the intra-peds void ratio e_m, whereas the volume of the pores having a radius greater than the threshold, referred to the volume of solids, measures the macrostructural void ratio e_M:

$$e_m = \frac{V_{vm}}{V_s},\ e_M = \frac{V_{vM}}{V_s}, \quad (1)$$

where V_{vm} is the volume of the intra-peds pores, V_{vM} is the volume of the macropores and V_s is the volume of the solids. Adequate corrections were carried out to account for very large and very small pores not intruded during the porosimetry tests (see Azizi et al., 2018 for the details). The total void ratio e is then:

$$e = e_m + e_M \quad (2)$$

By adopting such a double structure framework, the total water content can be determined as the sum of the water content within the peds and the water content within the macropores.

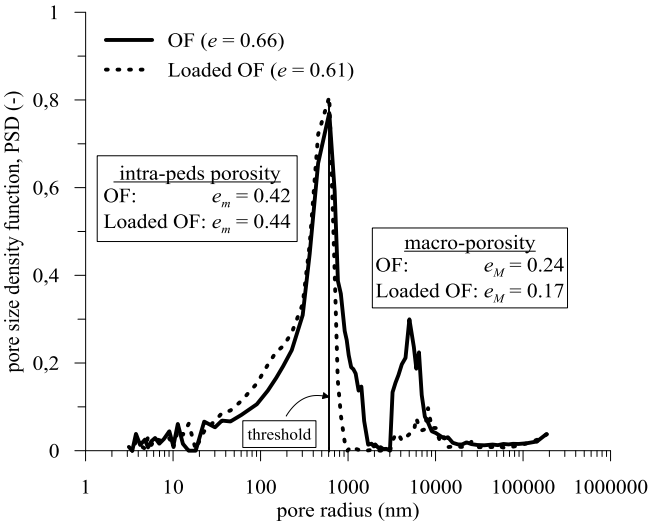

(a)

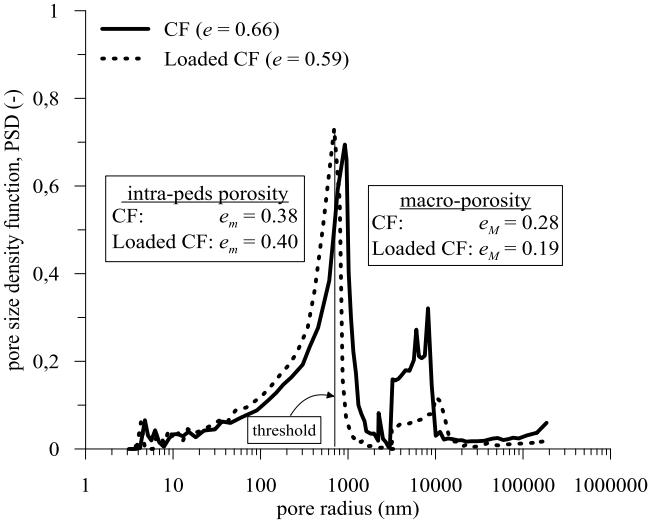

(b)

Figure 3. Evolution of PSD being subjected to mechanical load: (a) OF and loaded OF samples (b) CF and loaded CF samples.

Table 1. Conditions of samples at the beginning of shearing

Test	Fabric	Suction (kPa)	Mean net stress (kPa)	Water ratio e_w
TxOF01	OF	50	100	0.48
TxOF02	OF	50	200	0.48
TxOF03	OF	50	400	0.47
TxOF04	OF	300	100	0.36
TxCF01	CF	50	100	0.41
TxCF02	CF	50	200	0.42
TxCF03	CF	50	400	0.41
TxCF04	CF	300	100	0.25

By referring to the respective water ratios (e_{wM} and e_{wm} are water ratio of macropores and peds, respectively), it follows that:

$$e_w = e_{wM} + e_{wm} = e_M S_{rM} + e_m S_{rm} \quad (3)$$

where $e_{wm} = \frac{V_{wm}}{V_s}$, $e_{wM} = \frac{V_{wM}}{V_s}$, $S_{rm} = \frac{V_{wm}}{V_{vm}}$, $S_{rM} = \frac{V_{wM}}{V_{vM}}$, V_{wm} is the volume of water within the peds, V_{wM} is the volume of water within the macropores, S_{rm} is the intra-peds degree of saturation, S_{rM} is the macrostructural degree of saturation.

According to the data in Figure 3, drying-wetting cycles did not change the total void ratio. In spite of that, the macrostructural void ratio increased and the intra-peds void ratio decreased. Under mechanical loads, the CF sample was more compressible than the OF sample. For both samples, e_m remained almost constant while e_M decreased.

4 TRIAXIAL TESTS

Triaxial tests were carried out on both OF and CF samples. First, the samples were subjected to the desired suction (50 kPa or 300 kPa) by means of axis translation technique. They were held to equalise at constant suction until the changes in water content and volume stabilised. As the imposed suction was higher than the initial one, all samples dried. Consistently with their higher macro-porosity and larger pore sizes, CF samples showed a reduced water retention capacity (Azizi et al., 2018) and expelled more water than OF samples. Afterwards, the suction was kept constant and the mean net pressure was increased to the target values (100, 200 or 400 kPa) under free drainage condition. As already stated from the MIP results, CF samples were more compressible than OF samples: their void ratios at the end of consolidation were smaller than the ones of the OF samples under the same mean net stress. Finally, the samples were sheared under constant water content conditions by increasing the axial stress at open air drainage and closed water drainage, and the suction was measured. Table 1 provides the condition of the triaxial samples at the beginning of shearing.

5 SHEARING BEHAVIOUR

The experimental results were interpreted by elaborating the data using a modified Bishop effective stress, similar to the proposal of Alonso et al. (2010). It was assumed that the influence of suction on the effective stress could be weighted by the macrostructural degree of saturation, hence:

$$p'_M = p_{net} + S_{rM} s \quad (4)$$

where p'_M and p_{net} are the mean macroscopic effective stress and the mean net stress, respectively. It was further assumed that all the recorded volume strain is related to changes of e_M. The peak (hollow symbols) and ultimate (black symbols) data of the eight tests are shown in Figure 4. Samples tested at

higher suction and CF samples showed higher peak strengths.

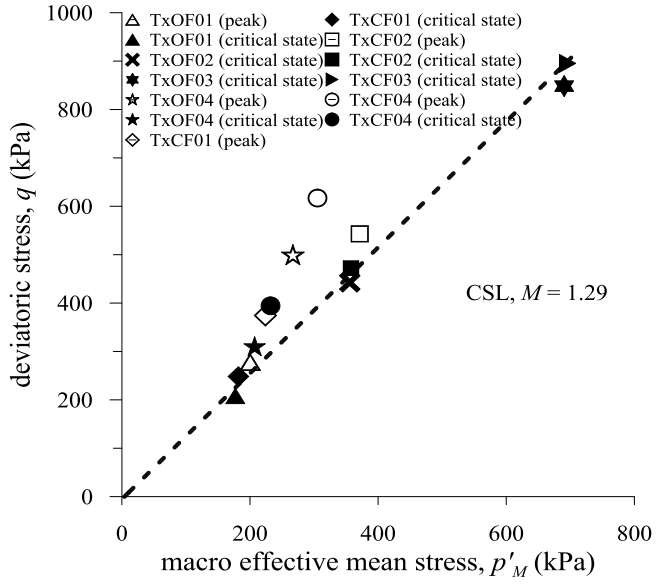

Figure 4. Peak and ultimate conditions in terms of deviatoric stress and macroscopic effective stress.

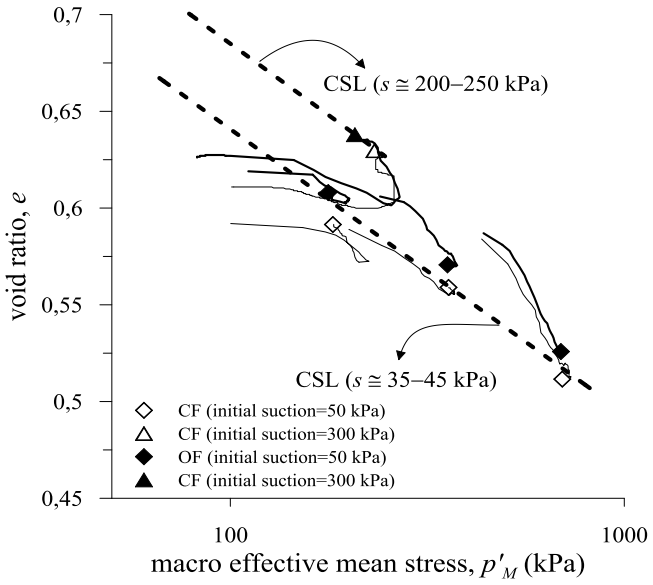

Figure 5. Critical state in terms of void ratio and macroscopic effective stress.

The ultimate conditions at the end of the tests approached the critical state. It can be appreciated that the slope of the critical state line, M = 1.29, is quite the same for the two data sets: furthermore, it is consistent with what obtained for saturated Viadana silt by Nocilla et al. (2006).

In the compression plane (Figure 5), one critical state line was determined for samples with initial suction s = 50 kPa and another one was adopted for samples with initial suction s = 300 kPa.

6 MODELLING

6.1 *Suction Changes*

A double structure water retention frame proposed by Azizi et al. (2018) was used to predict suction changes during shearing. For each structural level (linked to the intra-peds void ratio or to the macrostructural void ratio) the model employs one van-Genuchten relationship for main drying and another for main wetting. In terms of water ratio, the water retention curve of the soil is given by the sum of the water retention of the intra-peds and of the macropores:

$$e_w = e_M \left[\frac{1}{1+(\alpha_M s)^{n_M}}\right]^{m_M} + e_m \left[\frac{1}{1+(\alpha_m s)^{n_m}}\right]^{m_m} \quad (5)$$

where n_M, m_M, α_M and n_m, m_m, α_m are the parameters of van Genuchten (1980) model for macropores and intra-peds pores, respectively.

For each structural level, the air entry value is set to be dependent on its void ratio:

$$1/\alpha_M = (e_{M0}/e_M)^{\beta_1}/\alpha_{M0} \quad (6)$$

$$1/\alpha_m = (e_m/e_{m0})^{\beta_2}/\alpha_{m0} \quad (7)$$

where e_{M0} and e_{m0} are the macrostructural and intra-peds void ratios after compaction and $1/\alpha_{M0}$ and $1/\alpha_{m0}$ are the corresponding air-entry values of the drying curves. β_1 = 4 and β_2 = 9 were found to adequately reproduce the experimental results.

The state between the main drying and main wetting curves is described by scanning curves:

$$\Delta e_w^{sc} = \Delta e_{wM} + \Delta e_{wm} = \left[\frac{e_{wM}}{e_M}\Delta e_M - e_M k_{sc}\Delta s\right] + \left[\frac{e_{wm}}{e_m}\Delta e_m - e_m k_{sc}\Delta s\right] \quad (8)$$

where k_{sc} = 3×10^{-4} kPa^{-1} controls the slope of the scanning curves. The parameters of the water retention model used for the simulation are summarised in Table 2.

Table 2. Parameters of the water retention model

Parameters	$1/\alpha_{M0}$ (kPa)	n_M	m_M	$1/\alpha_{m0}$ (kPa)	n_m	m_m
Drying	64	1.75	0.83	263	2.86	0.14
Wetting	8	2.37	0.97	34	2.61	0.12

Since no water exchange took place during shearing, the water ratio e_w was constant, and suction changes occurred only through volume strains that were all referred to changes of e_M. Suction changes within the scanning domain can be predicted as:

$$\Delta s = \frac{e_{wM}}{e_M}\frac{\Delta e_M}{k_{sc} e_M} \quad (9)$$

Accordingly, an increase of e_M causes an increase in suction (mechanical drying), while a decrease of e_M causes a decrease of suction (mechanical

wetting). If void ratio changes are large enough, the hydraulic state reaches the main drying, or main wetting, branches. Under this condition, any volume change will cause a suction change, which can be predicted by coupling eq. (5) and eq. (6). Because of the dependency of the air entry value on the macrostructural void ratio, the main branches of the water retention curves shift towards lower suctions as the void ratio increases, whereas they shift toward higher suctions when the void ratio decreases. Thus, according to this model, a void ratio increase causes suction increase along scanning and suction decrease on the main branches. A void ratio decrease, instead, causes suction decrease along scanning and suction increase on the main branches.

Figure 6 compares the predictions of the model with the experimental results for samples sheared at confining net stress σ_{3net} = 100 kPa and initial suction s = 50 kPa. Their initial hydraulic state was close to the main wetting curve, but always remained within the scanning domain. The smaller suction decrease experienced by the CF samples is caused by their lower e_{wM} and higher e_M compared to the OF samples.

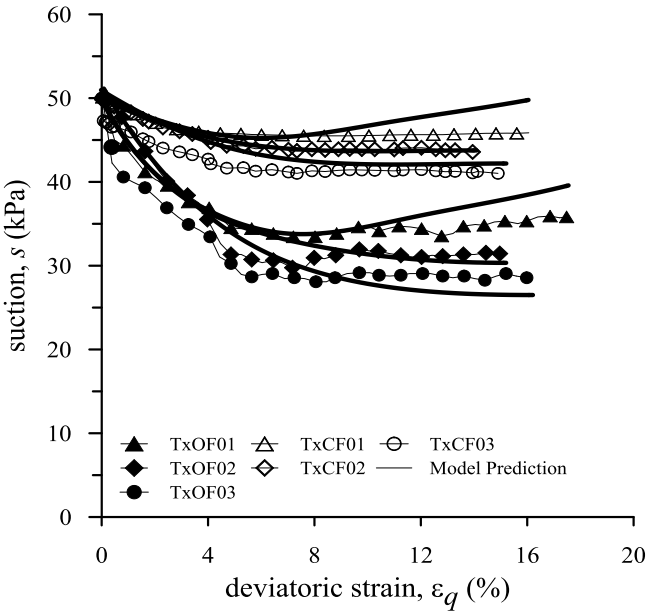

Figure 6. Suction values measured during shearing and model predictions (initial suction = 50kPa).

6.2 *Mechanical behaviour*

To investigate the role of fabric and suction on the shearing behaviour, reference was made to the Li and Dafalias (2000) stress-dilatancy relationship:

$$d = \frac{\partial \varepsilon_v}{\partial \varepsilon_q} = d_0 \left(e^{m\psi} - \frac{\eta}{M} \right) \tag{10}$$

where $\eta = q / p'$ is the stress ratio, d_0 and m are model parameters and ψ is the state parameter (Been and Jefferies 1985):

$$\psi = e - e_c(p') \tag{11}$$

where e_c is the void ratio at critical state for the given mean stress. Li and Dafalias relationship was inverted to predict the evolution of the stress ratio with deviatoric strain. Experimental values of dilatancy (Figure 7) were used as an input in the simulation. The saturated effective stress p' was substituted by the macroscopic effective stress p'_M in the definition of η to account for unsaturated conditions, in which the suction predicted by the water retention model was employed for its evaluation. The model predictions are compared to the experimental data in Figure 8 (original fabric) and Figure 9 (cycled fabric). In general, the peak stress ratio occurred in correspondence of the maximum dilatancy (minimum d), which was correctly reproduced by the model. The samples sheared at higher suction experienced larger dilatancy, which also is responsible for higher peak strength, as also found by Ng et al. (2017).

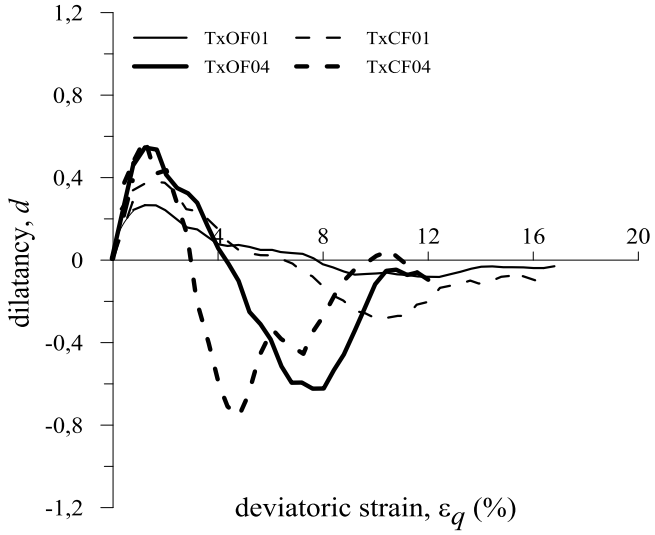

Figure 7. Dilatancy with respect to deviatoric strain.

Eventually, the model was improved by setting a dependency of d_0 on suction, which is consistent with the proposal of Chiu and Ng (2003), originally formulated with respect to net stresses. The law introduced for the dependency reads:

$$d_0 = d_{0*} + a \cdot log\ s \tag{12}$$

To account for the higher dilatancy (smaller d values) of CF samples (Figure 7), different values of m were used for the two fabrics. Table 3 provides the parameters used in the simulations.

Table 3. Parameters of the mechanical model

Parameters	M	m	d_{0*}	a
OF	1.29	8	0.6	0.5
CF	1.29	2	0.6	0.5

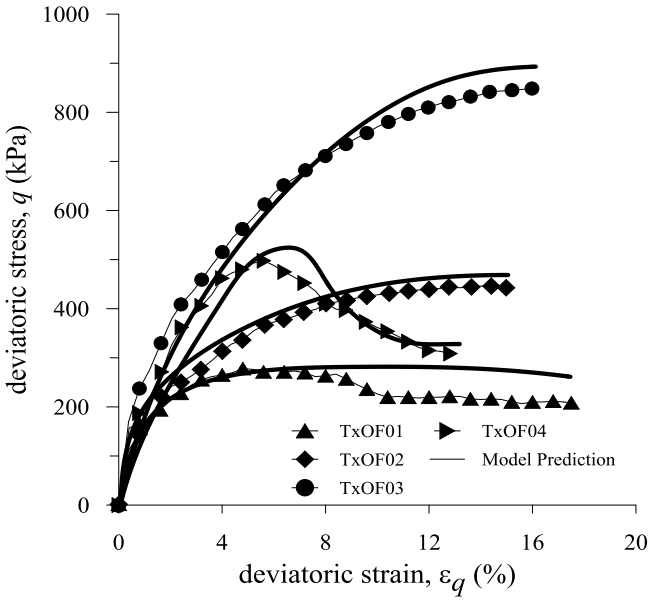

Figure 8. Shearing behaviour of OF samples: experimental data and model predictions.

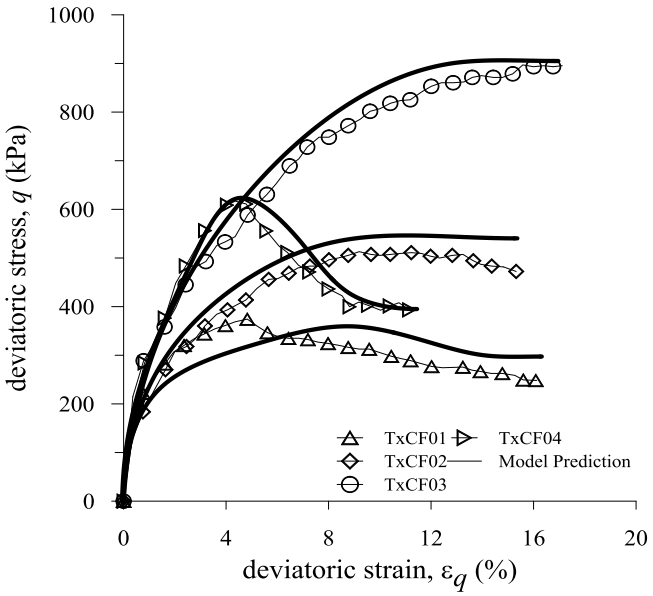

Figure 9. Shearing behaviour of CF samples: Experimental data and model predictions.

7 CONCLUSIONS

The results of the experimental work described in this paper suggest that the fabric of compacted non-active clayey silts can evolve significantly upon exposure to drying-wetting cycles, such as those expected to occur in continental climates. Superficial soil layers of earth structure soon show a different behaviour from the one expected at the time of construction.

As for the material tested in this study, drying-wetting cycles induced a larger macro-porosity. This promoted a more dilatant behaviour, and peak strengths higher than those of samples with the original fabric. Nevertheless, suction changes during shearing at constant water content were smaller for cycled samples, as explained by introducing a water retention model accounting for fabric changes. Dilatancy was found to increase with suction in both cases. The proposed extension of the Li and Dafalias stress – dilatancy relationship, originally proposed for saturated soils, was found to simulate well the shearing behaviour of all samples when using a Bishop type effective stress only related to the macro-porosity. To reproduce the experimental results adequately, a dependency of the parameters of the stress–dilatancy relationship on suction and fabric was required.

8 REFERENCES

Albrecht, B. & Benson, C. 2001. Effect of desiccation on compacted natural clays. *Journal of Geotechnical and Geoenvironmental Engineering*, 1271, 67–76.

Alonso, E., Pereira, J.M., Vaunat, J. & Olivella, S. 2010. A microstructurally based effective stress for unsaturated soils. *Géotechnique*, 60(12): 913–925.

Azizi, A., Musso, G. & Jommi, C. 2018. Effects of repeated hydraulic loads on microstructure and hydraulic behaviour of a compacted clayey silt. Submitted to *Géotechnique*.

Been, K. & Jefferies, M. G. 1985. A state parameter for sands. *Géotechnique*, 35(2), 99–112.

Benson, C. H., Sawangsuriya, A., Trzebiatowski, B. & Albright, W. H. 2007. Postconstruction changes in the hydraulic properties of water balance cover soils. *Journal of Geotechnical and Geoenvironmental Engineering*, 133(4), 349–359.

Calabresi, G., Colleselli, F., Danese, D., Giani, G. P., Mancuso, C., Montrasio, L., Nocilla, A., Pagano, L., Reali, E. & Sciotti A. 2013. A research study of the hydraulic behaviour of the Po river embankments. *Canadian Geotechnical Journal*, 50, 9, 947-960.

Chiu, C. F. & Ng, C. W. W. 2003. A state-dependent elasto-plastic model for saturated and unsaturated soils *Géotechnique* 53, No. 9, 809–829.

Delage, P. & Pellerin, F.M. 1984. Influence de la lyophilisation sur la structure d'une argile sensible du Québec. *Clay Minerals*, 19, 151-160.

Gallipoli D., Gens A., Sharma R. & Vaunat J. 2003. An elasto-plastic model for unsaturated soil incorporating the effects of suction and degree of saturation on mechanical behaviour. *Géotechnique*, 53(1):123–135.

Li, X. S. & Dafalias, Y. F. 2000. Dilatancy for cohesionless soils. *Géotechnique* 50, 4, 449–460.

Ng C. W. W., Sadeghi H. and Jafarzadeh F. 2017. Compression and shear strength characteristics of compacted loess at high suctions *Canadian Geotechecnical. Journal* 54: 690–699.

Nocilla, A., Coop, M. R. & Colleselli, F. 2006. The mechanics of an Italian silt; and example of "transitional" behaviour. *Géotechnique*, 56, No. 4, 261–271.